New Method for Regulating the Activity of ABO$_3$ Perovskite Catalysts

S. N. Vereshchagin[a], *, L. A. Solov'ev[a], E. V. Rabchevskii[a], V. A. Dudnikov[b], S. G. Ovchinnikov[b], and A. G. Anshits[a]

[a] *Institute of Chemistry and Chemical Technology, Siberian Branch, Russian Academy of Sciences, Krasnoyarsk, 660036 Russia*
[b] *Kirenskii Institute of Physics, Siberian Branch, Russian Academy of Sciences, Krasnoyarsk, 660036 Russia*
*e-mail: snv@icct.ru
Received November 4, 2014

Abstract—A new possibility of changing the activity and selectivity of perovskite catalysts in the oxidative conversion of methane was demonstrated using the $Sr_xGd_{1-x}CoO_{3-\delta}$ ($0.5 < x < 0.9$) compounds as an example. It was established that, at the same chemical composition, the disordering of Sr^{2+}/Gd^{3+} ions over the A positions of the crystal structure led to a significant increase in activity in the deep oxidation reaction of CH_4, as compared with the samples with an ordered distribution of cations.

Keywords: perovskite, cobalt, methane, deep oxidation, oxidative condensation

DOI: 10.1134/S0023158415040199

INTRODUCTION

Substituted rare-earth perovskites with the general formula $Ln_xA_{1-x}BO_{3-\delta}$ (Ln is a rare-earth element; A is Ca, Sr, or Ba; B is Mn, Co, Fe, or Ni; and **δ** is the oxygen off-stoichiometry index) are promising systems with uncommon electrical, magnetic, and optical properties [1]. They exhibit significant activity in different catalytic reactions, such as the deep and partial oxidation of hydrocarbons [2–4] and the conversion of hydrocarbons to CO and H$_2$ [5]. Their applications to the preparation of the oxygen-conducting membranes of reactors [6–8] and use in electrocatalytic and photocatalytic processes and fuel cells [9, 10] have been actively studied.

The activity of perovskites in the above catalytic reactions is primarily due to the structure peculiarities of these compounds.

In the ideal undistorted structure of perovskite, bulkier cations of the A type are surrounded by 12 anions in a cuboctahedral coordination, and smaller cations of the B type are surrounded by 6 anions in an octahedral coordination (Fig. 1a). The great possibilities of varying the nature of A and B cations and the formation of the mixed perovskites $Ln_xA_{1-x}B_yB'_{1-y}O_3$ are responsible for the variety of catalytic reactions with the participation of these systems.

The following factors responsible for the activity and selectivity levels of perovskites in the oxidative conversions of hydrocarbons can be recognized:

—the presence of oxygen vacancies [11];

—the ease of the removal of oxygen from the surface or lattice, the strength of Ln–O and Co–O bonds, and reducibility [12, 13];

—the structure of electron levels near the Fermi level, and the *d* level population and electronic configuration of the transition metal B [14];
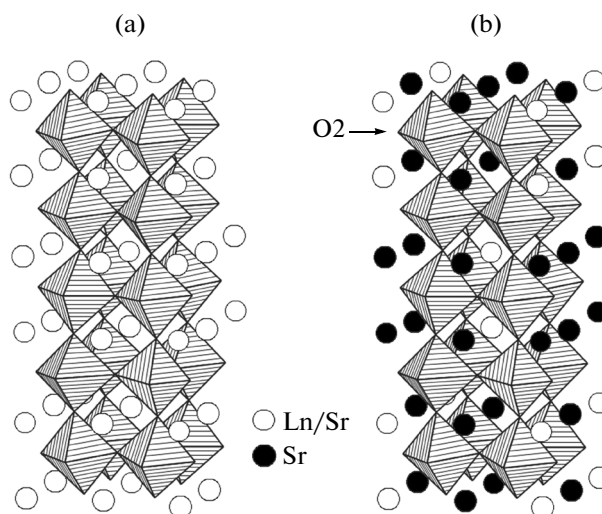

Fig. 1. (a) Ideal cubic structure and (b) structure of the mixed perovskite $Ln_xSr_{1-x}CoO_{3-\delta}$ (Ln = Sm, Gd, Dy, Y, Ho, Er, Tm, and Yb) ordered with respect to the A positions [17]. Light and dark circles designate the A positions, and octahedrons correspond to the positions of B cations. Oxygen ions/anionic vacancies are located at the apexes of octahedrons, and the label O2 indicates the site of the preferred localization of an oxygen vacancy in the ordered structure.

—the σ*-orbital population (e_g) and the degree of covalence of the transition metal B−oxygen bond [15];

—the presence of a microdomain structure caused by a morphotropic phase transition in the subsurface layers of LaSrCoO perovskites [16].

Most researchers believe that the catalytic activity of the perovskites $Ln_xA_{1-x}BO_{3-\delta}$ in reactions with the participation of oxygen is primarily related to the nature of the B cation and to the possibility of heterovalent substitution in the A position (for example, La^{3+} for Sr^{2+}). As a result of the replacement of the A cation, the valence state of the B cation changes within certain limits and anionic vacancies appear in the crystal lattice; this makes it possible to fine-tune the activity of perovskites.

At the same time, in the formation of double perovskites based on rare earth and alkaline earth metals, the distributions of Ln and A cations over crystal lattice positions can be different, depending on the ratio between the ionic radii and the conditions of the thermal treatment of samples. For example, it is well known [17] that the equilibrium distribution of cations over the A structure crystallographic positions in the $Ln_xSr_{1-x}CoO_{3-\delta}$ systems can vary from a completely disordered (random) distribution (for Ln = La−Nd) to an ordered distribution with the formation of a superlattice for the ions whose radius is smaller than that of Nd^{3+} (Fig. 1b).

Theoretical and experimental data suggest that, as a rule, in the case of cobaltates, the ordering of cations in the A position is also accompanied by the ordering of oxygen vacancies and a change in their mobility [18], which can affect the catalytic activity of these compounds in reactions with the participation of oxygen. By now, extensive experimental data on the interrelation of the nature of A and B cations with the catalytic properties of perovskites have been accumulated. However, data on the effect of the distribution of cations in the A position of the crystal structure on the catalytic behavior of these systems are almost absent from the literature. Recently, it was found that the catalytic activity of the single-phase compound $Gd_{0.2}Sr_{0.8}CoO_{3-\delta}$ in the deep oxidation reaction of methane was much higher with a disordered (random) distribution of Gd/Sr cations than in the case of a sample with an ordered arrangement of the Gd^{3+} and Sr^{2+} cations in the A position [19].

The aim of this work was to study the effect of the distribution of catalytically inert cations in double perovskites on their catalytic activity. This will make it possible to improve the currently available materials and to develop new perovskite materials (catalysts, chemical sensors, and oxygen-conducting membranes).

EXPERIMENTAL

The $Sr_xGd_{1-x}CoO_{3-\delta}$ ($0.5 \leq x \leq 0.9$) compounds were used in this study. This system was chosen because the synthesis procedure and the structure of the ordered $Sr_xLn_{1-x}CoO_{3-\delta}$ ($0.67 \leq x \leq 0.9$, Ln−Sm−Yb) compound were reported earlier [17], and rare-earth element cobaltates are well-known catalysts for the oxidative conversion of hydrocarbons.

The synthesis of $Sr_xGd_{1-x}CoO_{3-\delta}$ was carried out in accordance with a traditional ceramic technology by the multiple repetition of grinding−calcination (at 1200°C in air for 12 h) cycles with the starting mixture and the product obtained after calcination until the formation of a single-phase sample. Then, the samples were subjected to the following two different treatments:

(1) The sample was slowly cooled (annealed) in air from 1200 to 800°C at a rate of 2 K/min and was then held at 500°C to stabilize the oxygen content. This treatment led to the formation of an annealed sample.

(2) The sample was rapidly cooled (quenched) in air from 1200 to 800°C at a rate of about 30 K/s and was then held at 500°C to stabilize the oxygen content. This treatment led to the formation of a quenched sample.

In the subsequent text, the samples subjected to treatments 1 and 2 will be referred to as y-$Sr_xGd_{1-x}CoO_{3-\delta}$ and p-$Sr_xGd_{1-x}CoO_{3-\delta}$, respectively.

The resulting ceramic materials were crushed to a fraction of 0.1−0.16 mm for catalytic studies. The specific surface area of the samples calculated from data on the low-temperature adsorption of nitrogen (multipoint BET method) was 0.07−0.1 m^2/g.

Catalytic properties were studied in a semiautomatic microcatalytic flow system in a fixed-bed quartz reactor; the catalyst sample weight was 100 mg. The compositions of the initial mixture and conversion products were analyzed with the use of an Agilent 7890A multicolumn chromatograph (Agilent Technologies, United States). All of the samples were studied in the oxidative conversion of methane in a mixture of 15−82 vol % CH_4, 5−30 vol % O_2, and balance He over a temperature range of 350−850°C. The rates of deep oxidation were calculated for the points at which the conversion of the limiting component did not exceed 10%. The performance stability and the steady state of the catalyst were confirmed by the coincidence of the kinetic curves recorded in passing through the temperature range while increasing and decreasing the temperature.

The X-ray diffraction analysis was performed with the use of an X'Pert PRO diffractometer (PANalytical, Netherlands, CoK_α radiation); the measurements were carried out in an HTK 1200N high-temperature cell (Anton Paar, Austria) at $2\theta = 10°−140°$. X-ray structural data were obtained with the use of the full-
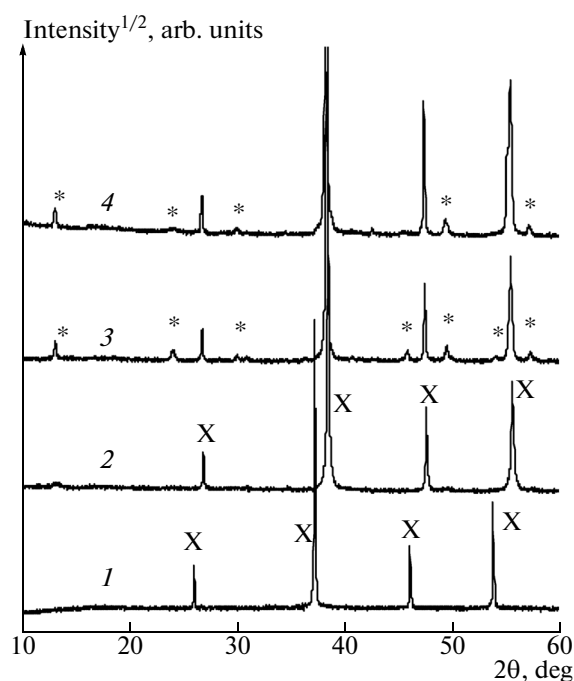
Intensity$^{1/2}$, arb. units

Fig. 2. X-ray diffraction patterns of the samples of (*1*) $Sr_{0.8}Gd_{0.2}Co_{3-\delta}$, $T_{an} = 1200°C$; (*2*) quenched $Sr_{0.8}Gd_{0.2}Co_{3-\delta}$, $T_{an} = 25°C$; (*3*) annealed $Sr_{0.8}Gd_{0.2}Co_{3-\delta}$, $T_{an} = 25°C$; and (*4*) annealed $Sr_{0.9}Gd_{0.1}Co_{3-\delta}$, $T_{an} = 25°C$ (T_{an} is the diffraction pattern recording temperature). X and * indicate the reflections from the cubic perovskite structure and the superstructure reflections of the tetragonal perovskite, respectively.

profile analysis of polycrystalline substances by derivative difference minimization [20].

The study of the samples by differential scanning calorimetry (DSC) and temperature-programmed reduction (TPR) with hydrogen was carried out on an STA 449C instrument (NETZSCH, Germany) coupled with an Aeolos QMS 403C mass spectrometer. The experiments were performed in a dynamic atmosphere with a controlled composition (Ar, O_2–Ar, and H_2–Ar) in platinum crucibles with 25–30 mg samples at a heating rate of 10 K/min.

RESULTS AND DISCUSSION

Phase Composition and Structure of $Sr_xGd_{1-x}CoO_{3-\delta}$

The X-ray diffraction analysis of the quenched and annealed samples of $Sr_xGd_{1-x}CoO_{3-\delta}$ ($0.5 \leq x \leq 0.9$) showed that all of the catalysts were single-phase ceramic materials, in which the effects of temperature and thermal treatment type on the phase state were similar regardless of the strontium content.

At a temperature of 1200°C, the cubic (*Pm*-3*m*) perovskite phase (Fig. 2, curve *1*) with a uniform random distribution of Sr^{2+}/Gd^{3+} ions and anionic vacancies in the appropriate crystal lattice positions (Fig. 1a) is stable at all strontium concentrations.

Quenching from 1200 to 500°C led to the retention of the cubic form (*Pm*-3*m*), and the metastable phase formed remained unchanged up to room temperatures for the samples with $x = 0.8$ and 0.9 (Fig. 2, curve *2*). For the quenched sample with $x = 0.5$, a number of phase transitions with a reduction of symmetry were observed at temperatures lower than ~500°C. X-ray diffraction analysis showed that the high-temperature and quenched forms of p-$Sr_xGd_{1-x}CoO_{3-\delta}$ are disordered cubic nonstoichiometric perovskite in the structure of which all A positions are equivalent and Sr/Gd atoms are randomly (statistically) distributed over them. All of the oxygen positions are also equivalent, whereas anionic vacancies are distributed randomly. The metastable phases formed remained unchanged up to 850°C in the presence of oxygen at concentrations of 2–20 vol %.

The annealed samples exhibited a more complicated behavior. The shape of DSC curves on the slow cooling of catalysts with $x = 0.9$ and 0.8 indicates the occurrence of a reversible exothermic process. The X-ray diffraction patterns of the annealed samples exhibited additional superstructure reflections (Fig. 2, curves *3*, *4*). The heating of the samples in a mixture of 20 vol % O_2–Ar was accompanied by an endothermic peak in the DSC curves (at 1174, 1113, or ~990°C for $x = 0.5$, 0.8, or 0.9, respectively) and by the disappearance of a superlattice structure. On this basis, we concluded that a phase transition occurs in the $Sr_xGd_{1-x}CoO_{3-\delta}$ system in a range of 990–1170°C; this phase transition consists in a redistribution of Sr and Gd cations and anionic vacancies in the material, and this process depends on the strontium content.

The slow cooling of the sample with $x = 0.5$ was accompanied by a decrease in the lattice symmetry, which is manifested in the complex *hkl*-dependent broadening of X-ray diffraction peaks and the appearance of additional superstructure reflections. The diffraction pattern of the material formed in this case cannot be described by a single crystal lattice; this fact is indicative of the possible phase separation caused by the nonuniform distribution of Sr and Gd atoms in the bulk of the material.

The annealing of the sample with $x = 0.8$ led to the conversion of a high-temperature cubic perovskite structure with the uniform random distribution of Sr and Gd into a phase with the ordered positions of Gd and localized oxygen vacancies and the formation of a tetragonal superlattice (Fig. 1b), which was described by James et al. [17].

Upon the slow cooling of the sample with $x = 0.9$, a new tetragonal phase was also formed as a result of the partial ordering of Sr^{2+}/Gd^{3+} cations and anionic vacancies, as evidenced by the appearance of additional superstructure reflections (Fig. 2, curve *4*). X-ray diffraction analysis showed that this phase differs from its analogues with $x = 0.5$ and 0.8 in terms of symmetry and ordering.

Physicochemical and catalytic properties of the ordered (y) and disordered (p) forms of the Sr$_x$GdGd$_{1-x}$CoO$_{3-\delta}$ catalysts

Structure	x	δ	n_{wbo}, mg/g	$T_{transition}$*, °C	lnk_{650}	X_{850}, %	S_{850}, %
y	0.8	0.37	0.4	~990	3.09	44	14.8
	0.9	0.33	1.4	1113	3.19	58	12.2
p	0.8	0.29	6.2	−	4.69	91	8.0
	0.9	0.31	7.9	−	4.30	96	7.5

δ is the oxygen off-stoichiometry index; n_{wbo} is the amount of weakly bound oxygen with $T_{des} < 320$°C; k_{650} is the rate constant of deep oxidation ($10^8 \times$ mol g^{-1} s^{-1}) at 560°C; X_{850} and S_{850} are the conversion of oxygen and selectivity for the formation of C$_2$ hydrocarbons, respectively, at 850°C and a reaction mixture of CH$_4$: O$_2$: He = 27 : 13 : 60 (vol %).

* The temperature of a maximum rate of transition to a disordered cubic structure in a mixture of 20% O$_2$–Ar according to the DSC data at a heating rate of 10 K/min.

Thus, the difference between the quenched and annealed catalysts consists in different distributions of the Sr^{2+}/Gd^{3+} cations and anionic vacancies in the structure of perovskite. The quenched samples are disordered perovskites with the random distribution of Sr^{2+}/Gd^{3+} and oxygen vacancies over appropriate crystal lattice positions, whereas the annealed samples are characterized by a more or less ordered distribution of the Sr^{2+}/Gd^{3+} cations over the A positions of the structure, which is also accompanied by the ordering of oxygen vacancies. Because we failed to obtain a single-phase ordered sample with $x = 0.5$, we studied the effect of structure features on catalytic properties in the compositions with $x = 0.8$ and 0.9.

Catalytic Properties of Sr$_x$Gd$_{1-x}$CoO$_{3-\delta}$

The catalytic experiments showed that, at temperatures lower than 600–650°C, the deep oxidation reaction of methane occurred with the formation of CO$_2$. At $T > 700$°C, the contribution of the oxidative condensation of methane (OCM) with the formation of ethane and ethylene became noticeable. In this case, the activity of catalysts with the disordered distribution of cations was higher by a factor of 2–5 than the activity of systems with an ordered Sr/Gd distribution (see the table and Fig. 3). Thus, for the y-Sr$_{0.8}$Gd$_{0.2}$CoO$_{3-\delta}$ sample, the same conversion of

the reactants was reached at higher temperatures; as compared with p-Sr$_{0.8}$Gd$_{0.2}$CoO$_{3-\delta}$, the difference was about 150°C.

Because of the low specific surface areas of the catalysts, their total activity (per gram) in the reaction of complete oxidation was low; correspondingly, sufficiently high temperatures should be maintained. However, the calculated specific activity per square meter was comparable with published data on the activity of rare-earth element perovskites in the reaction of methane oxidation [22].

According to kinetic data, the deep oxidation reaction is first-order with respect to methane and is of fractional variable order with respect to oxygen (in the ranges of methane and oxygen partial pressures of 0.15–0.82 and 0.05–0.3 atm, respectively). The dependence of the rate of methane conversion on the concentrations of the reactants is adequately described by the equation

$$w_{CH_4} = kP_{CH_4}; \quad k = \frac{a\sqrt{P_{O_2}}}{1 + b\sqrt{P_{O_2}}}, \tag{1}$$

where w_{CH_4} and k are the rate and the rate constant of methane conversion, respectively; P_{O_2} and P_{CH_4} are the partial pressures of oxygen and methane, respectively; and a and b are equation constants.
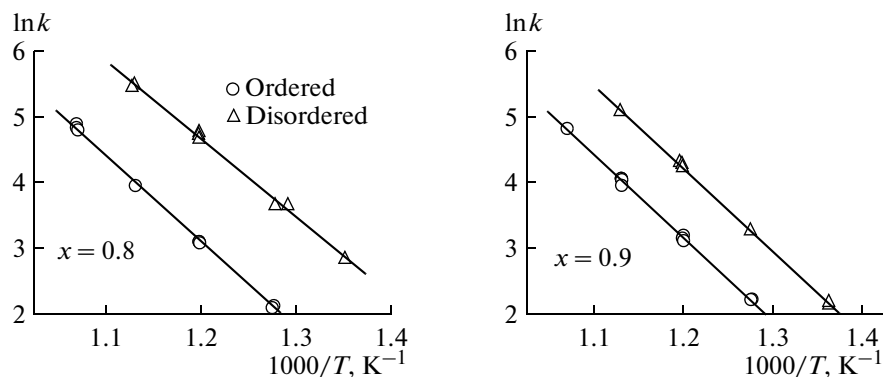

Fig. 3. Arrhenius plots for the reaction rate constant k of the deep oxidation of methane over ordered and disordered Sr$_x$Gd$_{1-x}$CoO$_{3-\delta}$ perovskites. Reaction mixture (vol %): CH$_4$: O$_2$: He = 27 : 13 : 60.

The plots of the logarithms of the rate constants as a function of the reciprocal of temperature (Fig. 3) suggest that the apparent activation energies of all of the samples are $100-110$ kJ/mol. The activity of the samples with a disordered structure was higher than the activity of the catalysts with an ordered structure at close apparent activation energies; this fact is indicative of an unchanged mechanism of conversion for all of the samples.

Note that the observed rates of methane oxidation in the presence of all of the test catalysts were stable in time, and the kinetic curves (and Arrhenius plots) were reproducible under repeatedly changed conditions (temperature and reactant concentrations). This is indicative of the absence of a transition from a metastable cubic structure to a stable tetragonal one under the conditions of catalysis at temperatures lower than $700°C$, at least, during the period of a catalytic experiment (several hours).

At $850°C$, the high conversion of the limiting component (oxygen), which was $40-99\%$, and the complex homogeneous−heterogeneous mechanism of the OCM reaction substantially hampered the kinetic analysis. However, the total activity of the samples with a disordered structure was also higher than the activity of the samples with an ordered structure (see the table). The initial selectivity for the formation of C_2 hydrocarbons was higher in the case of the samples with an ordered structure. This most likely occurred due to their lower activity in the deep oxidation reaction (see the table).

At high temperatures, the performance stability of the y-$Sr_{0.9}Gd_{0.1}CoO_{3-\delta}$ sample was low. The p-$Sr_{0.8}Gd_{0.2}CoO_{3-\delta}$ sample stably worked for 3 h; in this case, superstructure reflections did not appear in the X-ray diffraction pattern of the material after catalysis. In contrast to this sample, the selectivity of y-$Sr_{0.9}Gd_{0.1}CoO_{3-\delta}$ at $850°C$ rapidly decreased to approach the value of S_{850} for p-$Sr_{0.9}Gd_{0.1}CoO_{3-\delta}$ after a 3-h operation (see the table). The partial disordering of cations under the action of a reaction atmosphere at a decreased partial pressure of oxygen can be a possible reason for this; this is consistent with the lower temperature stability of the tetragonal ordered structure of y-$Sr_{0.9}Gd_{0.1}CoO_{3-\delta}$ (see the table) and the weakening of the intensity of superstructure reflections in the X-ray diffraction pattern of the y-$Sr_{0.9}Gd_{0.1}CoO_{3-\delta}$ sample after the oxidation reaction.

Thus, the above experimental data suggest that, at the same overall composition, strontium−gadolinium cobaltates with a statistical (random) distribution of the Sr/Gd atoms over the A positions of the perovskite crystal structure exhibit higher activity in the reaction of methane oxidation.

It is well known that the mobility of framework oxygen is one of the most important factors responsible for the activity of perovskite catalysts containing rare-earth elements. It is assumed that the regeneration of a catalytic center occurs due to mobile lattice oxygen on its diffusion from the depth of a crystal [4]. Borovskikh et al. [21] found that the mobility of oxygen ions in the structure is responsible for the oxidation of methane on $La_{1-x}Sr_xCoO_{3-\delta}$. The capacity of the $LaFeO_{3-\delta}$ phase for the deep oxidation of methane was attributed to the presence of oxygen vacancies in it and their ability to sorb considerable amounts of oxygen [22]. The activity of the $La_{1-x}Nd_xCoO_3$ system in the oxidation of CH_4 also correlates with the amount of mobile sorbed oxygen [23].

It is possible to assume that the change in the catalytic activity upon the ordering/disordering of catalytically inactive Sr/Gd cations in the test system is due to changes in the energy characteristics and mobility of framework oxygen. This possibility follows from the results of the theoretical calculations of the dependence of oxygen mobility in the framework of the compound $Ba_{0.5}Sr_{0.5}Co_{1-x}Fe_xO_{2.5}$ on the distribution of the Ba^{2+}/Sr^{2+} ions: the structures with an ordered arrangement of cations were characterized by lower diffusion coefficients of oxygen [18], and the ordering of cations was also accompanied by the ordering of oxygen vacancies.

The TPR curves given in Fig. 4 for the catalysts with ordered and disordered Sr/Gd distributions confirm the validity of the assumption made. A weakly bound low-temperature form of oxygen was present in the p-$Sr_xGd_{1-x}CoO_{3-\delta}$ samples (the concentration of this form in the y-$Sr_xGd_{1-x}CoO_{3-\delta}$ systems was small), and the amount of this form correlated with the activity of samples in the deep oxidation of methane and selectivity for the OCM reaction (see the table). The oxygen off-stoichiometry index δ is also indicative of a higher oxygen content of the p-$Sr_xGd_{1-x}CoO_{3-\delta}$ samples; this index was regularly lower in metastable systems disordered with respect to the A position (see the table).

Thus, the catalytic properties of the $Sr_xGd_{1-x}CoO_{3-\delta}$ system in the deep oxidation of methane and the OCM reaction depend significantly on the ordering of Sr^{2+}/Gd^{3+} cations in the A position of the perovskite structure. The systems with the disordered distribution of the Sr^{2+}/Gd^{3+} cations and oxygen vacancies are more preferable for the deep oxidation reaction of methane. The systems with localized oxygen vacancies and an ordered arrangement of the Sr^{2+}/Gd^{3+} cations ensure higher selectivity for the formation of C_2 products in the OCM reaction.

The experimental data on the structure and catalytic activity of single-phase gadolinium−strontium cobaltates with the structure of perovskite demonstrate a new method, which was not used earlier, for the regulation of the oxidizing activity of catalysts by changing the distribution of catalytically inert ions over the crystallographic A positions. It is most likely that the found regularities are of general nature; they are not limited to Sr−Gd cobaltates, and they can be used for improving currently available materials and developing new materials with the structure of perovs-
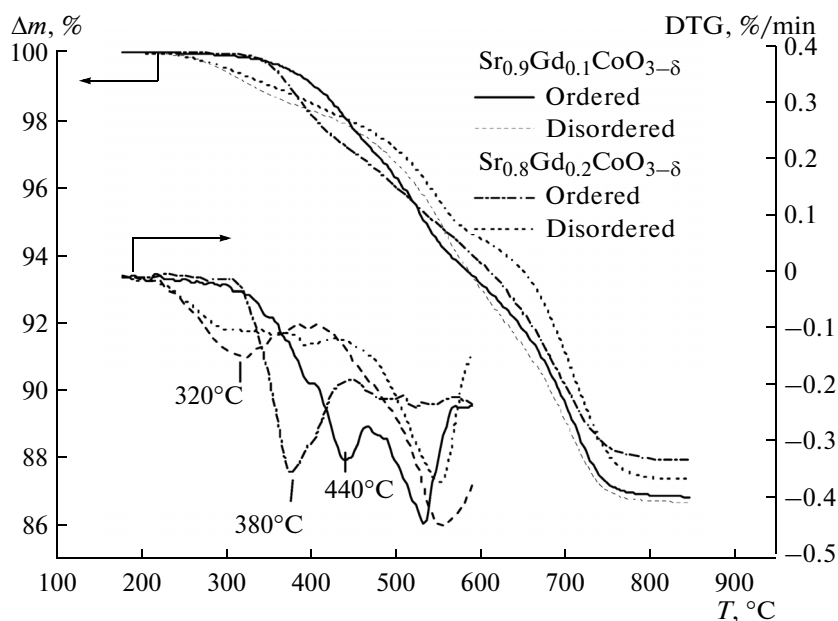
Fig. 4. TG and DTG curves for the temperature-programmed reduction of the $Sr_xGd_{1-x}CoO_{3-\delta}$ catalysts in ordered and disordered forms in a mixture of 5 vol % H_2-Ar; heating rate, 10 K/min.

kite, such as catalysts for processes with the participation of oxygen, oxygen-conducting membranes, and chemical sensors.

REFERENCES

1. Ivanova, N.V., Ovchinnikov, S.G., Korshunov, M.M., Eremin, I.M., and Kazak, N.V., *Phys. Usp.*, 2009, vol. 52, p. 789.

2. Falcón, H., Barbero, J.A., Alonso, J.A., Martínez-Lope, M.J., and Fierro, J.L.G., *Chem. Mater.*, 2002, vol. 14, p. 2325.

3. Yamazoe, N. and Teraoka, Y., *Catal. Today*, 1990, vol. 8, p. 175.

4. Pena, M.A. and Fierro, J.L.G., *Chem. Rev.*, 2001, vol. 101, p. 1981.

5. Nalbandian, L., Evdou, A., and Zaspalis, V., *Int. J. Hydrogen Energy*, 2009, vol. 34, p. 7162.

6. Bhatia, S., Thien, Ch.Y., and Mohamed, A.R., *Chem. Eng. J.*, 2009, vol. 148, p. 525.

7. Olivier, L., Haag, S., Mirodatos, C., and van Veen, A.C., *Catal. Today*, 2009, vol. 142, p. 34.

8. Tan, X., Pang, Z., Gu, Z., and Liu, S., *J. Membr. Sci.*, 2007, vol. 302, p. 109.

9. Jun, L., Ling, Z., and Guanzhong, L., *Ind. Eng. Chem. Res.*, 2009, vol. 48, p. 641.

10. Tao, S.W. and Irvine, J.T.S., in *Metal Oxides: Chemistry and Application*, Fierro, J.L.G., Ed., Boca Raton, Fla.: CRC, 2006, p. 739.

11. Falcón, H., Martínez-Lope, M.J., Alonso, J.A., and Fierro, J.L.G., *Appl. Catal., B*, 2000, vol. 2, p. 131.

12. Jiang, A., Peng, Y., Zhou, Q., Gao, P., Yuan, H., and Deng, J., *Catal. Lett.*, 1989, vol. 3, p. 235.

13. Futai, M., Yonghua, C., Louhui, L., *React. Kinet. Catal. Lett.*, 1986, vol. 31, p. 47.

14. Tejuca, L.G., Fierro, J.L.G., and Tascón, J.M.D., *Adv. Catal.*, 1989, vol. 36, p. 237.

15. Suntivich, J., Gasteiger, H.A., Yabuuchi, N., Nakanishi, H., Goodenough, J.B., and Shao-Horn, Y., *Nat. Chem.*, 2011, vol. 3, p. 546.

16. Isupova, L.A., Alikina, G.M., Tsybulya, S.V., Boldyreva, N.N., Kryukova, G.N., Yakovleva, I.S., Isupov, V.P., and Sadykov, V.A., *J. Inorg. Mater*, 2001, vol. 3, p. 559.

17. James, M., Cassidy, D., Goossens, D.J., and Withers, R.L., *J. Solid State Chem.*, 2004, vol. 177, p. 1886.

18. Shiiba, H., Bishop, C.L., Rushton, M.J.D., Nakayama, M., Nogami, M., Kilner, J.A., and Grimes, R.W., *J. Mater. Chem. A*, 2013, vol. 1, p. 10345.

19. Vereshchagin, S.N., Solovyov, L.A., Rabchevskii, E.V., Dudnikov, V.A., Ovchinnikov, S.G., and Anshits, A.G., *Chem. Commun.*, vol. 50, p. 6112.

20. Solovyov, L.A., *J. Appl. Crystallogr.*, 2004, vol. 37, p. 743.

21. Borovskikh, L., Mazo, G., and Kemnitz, E., *Solid State Sci.*, 2003, vol. 5, p. 409.

22. Belessi, V.C., Ladavos, A.K., and Pomonis, P.J., *Appl. Catal., B*, 2001, vol. 31, p. 183.

23. Taguchi, H., Matsuoka, S., Kato, M., and Hirota, K., *J. Mater. Sci.*, 2009, vol. 44, p. 5732.

Translated by V. Makhlyarchuik